Structure, Substitution and Hydrolysis of Bis(trifluorobenzoylacetonato-O,O')dichloro titanium(IV): an Experimental and Computational Study

Annemarie Kuhn,[a] Sonja Tischlik,[b] Kathrin H. Hopmann,[b,c*] Marilé Landman,[d] Petrus. H. van Rooyen[d] and Jeanet Conradie[a,c]*

[a] Department of Chemistry, PO Box 339, University of the Free State, 9300 Bloemfontein, Republic of South Africa. Tel: 27-51-4012194.

[b] Department of Chemistry, University of Tromsø, N-9037 Tromsø, Norway

[c] Center for Theoretical and Computational Chemistry (CTCC), University of Tromsø, N-9037 Tromsø, Norway

[d] Department of Chemistry, University of Pretoria, Private Bag X20, Hatfield, 0028, South Africa. Tel: 27-12-4202527.

*Contact author details:

Name: Jeanet Conradie

Tel: +27-51-4012194

Fax: +27-51-4446384

e-mail: conradj@ufs.ac.za

Structure, Substitution and Hydrolysis of Bis(trifluorobenzoylacetonato-O,O')dichloro titanium(IV): an Experimental and Computational Study

Annemarie Kuhn,[a] Sonja Tischlik,[b] Kathrin H. Hopmann,[b,c*] Marilé Landman,[d] Petrus. H. van Rooyen[d] and Jeanet Conradie[a,c]*

[a] Department of Chemistry, PO Box 339, University of the Free State, 9300 Bloemfontein, Republic of South Africa. Tel: 27-51-4012194, Fax: 27-51-4017295

[b] Department of Chemistry, University of Tromsø, N-9037 Tromsø, Norway

[c] Center for Theoretical and Computational Chemistry (CTCC), University of Tromsø, N-9037 Tromsø, Norway

[d] Department of Chemistry, University of Pretoria, Private Bag X20, Hatfield, 0028, South Africa. Tel: 27-12-4202527, Fax: 27-12-4204687

ABSTRACT

The chlorine coordinated ligands in $[Ti(tfba)_2Cl_2]$ (Htfba = 4,4,4-trifluoro-1-(phenyl)-1,3-butanedione = $PhCOCH_2COCF_3$) are very susceptible to hydrolysis and even with trace amounts of water, the formation of hydrolysed complexes, dinuclear $\{Ti(tfba)_2Cl\}_2(\mu\text{-}O)$ or tetranuclear $[Ti(tfba)_2(\mu\text{-}O)]_4$, take place, whereas with an excess of water, decomposition to TiO_2 occurs. Substitution of the chloro-ligands in $[Ti(tfba)_2Cl_2]$ with H_2biphen (H_2biphen = 2,2'-dihydroxybiphenyl or biphenol) leads to $[Ti(tfba)_2$biphen$]$ with enhanced water stability. Experimentally, two steps were observed for the substitution $[Ti(tfba)_2Cl_2]$ + H_2biphen. Computational chemistry calculations reveal that each step involves several transition states, with formation of a 7-coordinated intermediate in the first reaction half. Location of this intermediate is dependent on inclusion of empirical dispersion-corrections in the functional. The three geometrical *cis*-isomers of $[Ti(tfba)_2$biphen$]$ were observed in solution using low temperature ^{1}H and ^{19}F NMR, whereas in the solid state, two of the isomers, *cis-cis-trans* and *cis-*

trans-cis, crystallized in the same unit cell. The crystal structure of the hydrolysed tetranuclear complex $[Ti(tfba)_2(\mu\text{-}O)]_4$ is composed of four identical *cis-cis-trans* isomers of $[Ti(tfba)_2Cl_2]$. The eight β-diketonato backbones and the four bridging oxygens have a S_4 molecular symmetry.

Keywords

titanium; substitution; hydrolysis; beta-diketone

1 Introduction

Increasing knowledge of organometallic chemistry enables the design of new compounds with specific applications, *e.g*. in catalysis or in cancer therapy. Amongst the most well-known organometallic titanium(IV) complexes that show antitumour properties, are titanocene dichloride (bis(cyclopentadienyl)titanium(IV)dichloride) and budotitane ($[Ti(benzoylacetonato)_2OEt_2]$ or *cis*-diethoxybis(benzoylacetonato)titanium(IV)), see Figure 1 (a) and (b). The advantage of these Ti(IV) complexes over the *cis*-platin (*cis*-diamminedichloroplatinum(II)), the first metal complex possessing antitumour properties, is their biological compatibility resulting in milder side effects [1]. However, due to the electron-poor and oxophilic nature of these titanium(IV) complexes, hydrolysis occurs readily, leading to insoluble species such as $[Ti(benzoylacetonato)_2O]_2$ [2] and the eventual formation of TiO_2 [3]. This hydrolytic instability makes them unsuitable for therapeutic applications, initiating the need for more stable Ti(IV) complexes with well defined hydrolytic behaviour [4,5]. Derivatives of titanocene dichloride, such as bis-[(*p*-methoxybenzyl)-cyclopentadienyl] titanium(IV) dichloride (Titanocene Y, see Figure 1 (c)) are found to have improved activity against renal cell cancer [6].

A third family of cytotoxic Ti(IV) agents is the bis(isopropoxo)-Ti complexes with diamine bis(phenolato) ligands, also known as the salan complexes [7], see Figure 1 (d). These complexes showed distinctly improved hydrolytic stability and antitumor activity against colon HT-29 and ovarian OVCAR-1 cells compared to budotitane and titanocene dichloride [8,[9].

Bulky [10,11], as well as chelating electron-rich oxygen-based ligands such as salan [8,9] acetylacetonate and glycols [12], showed increased stability towards hydrolysis when coordinated to titanium. The activity of a metal complex against cancer is primarily related to the nature of the ligands and their substitution stability [13]. Knowledge of the structure and properties of titanium(IV) complexes are thus of importance and may lead to the design of new compounds with specific applications. In this contribution we present an experimental and computational chemistry study of the substitution reaction of the chlorides in $[Ti(tfba)_2Cl_2]$ (**1**) with a chelating electron-rich oxygen-based ligand H_2biphen (Htfba = 4,4,4-trifluoro-1-(phenyl)-1,3-butanedione or trifluorobenzoylacetone; H_2biphen = 2,2'-dihydroxybiphenyl or biphenol) to give $[Ti(tfba)_2biphen]$ (**2**), see Figure 1 (e) and (f). The solid state structure of $[Ti(tfba)_2biphen]$, as well as a hydrolysed product of the reactant, namely the tetranuclear complex $[Ti(tfba)_2(\mu\text{-}O)]_4$ are also presented.

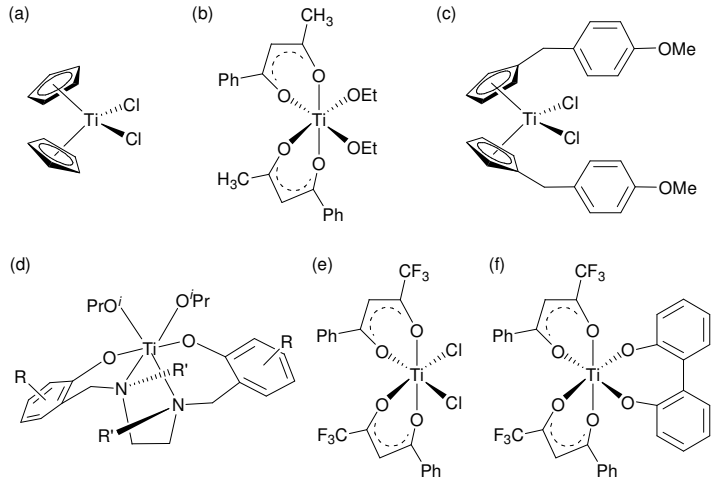

Figure 1. Structure of potential anticancer drugs (a) titanocene dichloride, (b) budotitane, (c) titanocene Y and (d) titanium-salan, and complexes of this study (e) $[Ti(tfba)_2Cl_2]$ (1) and (f) $[Ti(tfba)_2biphen]$ (2).

2 Experimental and Theoretical Methods

2.1 Apparatus

NMR measurements at 25 °C were recorded on a Bruker Avance II 600 NMR spectrometer [^{1}H (600.130 MHz)]. The chemical shifts were reported relative to $SiMe_4$ (0.00 ppm). Positive values

indicate downfield shift. UV/vis spectra were recorded on a Cary 50 Probe UV/vis spectrophotometer. Melting points are uncorrected and were determined with a Reichert Thermopan microscope fitted with a Koffler hot stage (up to 200 °C). Mass spectra were recorded on a SYNAPT G2 HDMS instrument, using electrospray ionization as the ion source and a time-of-flight mass analyser. A sampling time of 3 minutes was used, with the direct infusion inlet method.

2.2 Synthesis

Solid reagents used in preparations (Merck, Aldrich and Fluka) were used without further purification. Liquid reactants were distilled prior to use. Organic solvents were distilled and dried according to published methods [14]. All glassware was flame-dried and was allowed to cool in a stream of dry N_2. All operations were carried out under anhydrous conditions in a dry N_2 atmosphere. The N_2 atmosphere was maintained throughout the reaction. Filtrations and recrystallisations were performed under a blanket of N_2. The $[Ti(tfba)_2Cl_2]$ (**1**) and $[Ti(tfba)_2$biphen] (**2**) complexes were synthesized as reported previously [15]. A mixture of the mononuclear $[Ti(tfba)_2Cl_2]$ complex and the hydrolysed dinuclear $\{Ti(tfba)_2Cl\}_2(\mu$-O) complex (**3**) was observed when $[Ti(tfba)_2Cl_2]$ (**1**) was dissolved in $CDCl_3$, similar as previously observed for related $[Ti(\beta$-diketonato$)_2Cl_2]$ complexes containing a CF_3 group on the β-diketonato ligand in $CDCl_3$ solution [16]. The tetranuclear complex $[Ti(tfba)_2(\mu$-O$)]_4$ (**4**), formed from $[Ti(tfba)_2Cl_2]$ dissolved in deuterated chloroform and sealed in NMR tubes. Trace amounts of water in the deuterated chloroform (Sigma Aldrich, CAS Number 865-49-6, ≤ 0.01 % water) let to the formation of the hydrolyzed tetranuclear complex $[Ti(tfba)_2(\mu$-O$)]_4$ (**4**) in solution of $CDCl_3$.

Bis(trifluorobenzoylacetonato-O,O')dichlorotitanium(IV)

$[Ti(tfba)_2Cl_2]$ **(1)*:*** Yield 60 % (0.330 g). M.p. > 200 ˚C. Colour: orange. ^{1}H NMR (300 MHz, δ/ppm, $CDCl_3$): Monomer: 7.05 (s, 2H, 2x CH), 7.58 (t_{br}, 4H, 2x 2H, PhH), 7.77 (t_{br}, 2H, 2x 1H, PhH), 8.11 (br, 4H, 2x 2H, PhH). Dinuclear complex: 6.85 (s, 2H, 2x CH), 7.44 (br, 4H, 2x 2H, PhH), 7.63 (t_{br},

2H, 2x 1H, PhH), 8.02 (br, 4H, 2x 2H, PhH). ^{19}F NMR (600 MHz, δ/ppm, $CDCl_3$): Monomer and dimer: -73.44 – -75.43 (br, 6H, 2x CF_3)

Bis(trifluorobenzoylacetonato-O,O')(biphenyldiolato-O,O')titanium(IV)

[Ti(tfba)$_2$biphen] **(2):** Yield 58 % (0.3824 g). M.p. > 200 ˚C. Colour: red. ^{1}H NMR (600 MHz, δ/ppm, $CDCl_3$): 6.89 (s, 2H, 2x CH), 7.02 (d_{br}, 2H, biphenH), 7.16 (t, 2H, biphenH), 7.37 (t_{br}, 2H, biphenH), 6.47 (t, 4H, 2x 2H, PhH), 7.52 (d, 2H, biphenH), 7.64 (t, 2H, 2x 2H, PhH), 7.91 (d, 4H, 2x 2H, PhH). ^{19}F NMR (δ/ppm, $CDCl_3$): -75.03 (6F, br, CF_3). Elemental *Anal*. Calc. for $TiC_{32}H_{20}O_6F_6$: C, 58.0; H, 3.0. Found: C, 57.8; H, 3.0%. MS (m/z): $C_{32}H_{20}F_6O_6Ti$ Calc. 662.06 $[M]^+$, Exp. 663.07 $[M+H]^+$.

[Ti(tfba)$_2$(μ-O)]$_4$ **(4):** Colour: Yellow. ^{1}H NMR (600 MHz, δ/ppm, $CDCl_3$): 6.42 (s, 4H, 4x CH), 6.95 (t, 8H, 4x 2H, PhH), 7.16 (t, 4H, 4x 1H, PhH), 7.85 (d, 8H, 4x 2H, PhH). MS (m/z): $C_{80}H_{48}F_{24}O_{20}Ti_4$ Calc. 1976.03 $[M]^+$, Exp. 1977.03 $[M+H]^+$.

2.3 Kinetic measurements

The substitution reaction was monitored on the UV/vis (by monitoring the change in absorbance at the 450 nm) spectrophotometers. All kinetic measurements were monitored under pseudo-first-order conditions with [H_2biphen] 10 to 200 times the concentration of the [Ti(tfba)$_2$Cl$_2$] complex in CH_3CN solution. The concentration [Ti(tfba)$_2$Cl$_2$] ≈ 0.0001 mol dm^{-3}. Kinetic measurements, under pseudo-first-order conditions for different concentrations of [Ti(tfba)$_2$Cl$_2$] at a constant [H_2biphen], confirmed that the concentration of [Ti(tfba)$_2$Cl$_2$] did not influence the value of the observed kinetic rate constant. The pseudo-first-order rate constants, k_{obs}, were calculated by fitting [18] kinetic data to the first-order equation [17]: $A_t - A_\infty = (A_0 - A_\infty)\, e^{(-k_{obs} \times t)}$, with A_t , A_∞ and A_0 = the absorbance of the indicated species at time t, infinity and 0 respectively. The experimentally determined pseudo first order rate constant k_{obs} is converted to a second order rate constant, $k_{2(step\ 1)}$ (for the first reaction step), by determining the slope of the linear plot of k_{obs} against the concentration of the incoming biphenolato ligand. Non-zero intercepts implied that $k_{obs} = k_{2(step\ 1)}$[biphen] + k_s and that

the first order rate constant for a solvent pathway, k_s, in the proposed reaction mechanism exists. The first order rate constant for the second reaction step will be denoted by $k_{2(\text{step } 2)}$. All kinetic mathematical fits were done utilizing the fitting program MINSQ [18]. The error of all the data are presented according to crystallographic conventions, for example k_{obs} = 0.0243(2) s^{-1} implies k_{obs} = (0.0243 ± 0.0002) s^{-1}. The activation parameters were determined from the Eyring relationship [17] and the activation free energy $\Delta G^{\ddagger} = \Delta H^{\ddagger} - T\Delta S^{\ddagger}$.

2.4 Computational methods

All calculations were performed with the B3LYP functional as implemented in the Gaussian 09 package [19], in combination with the Grimme empirical dispersion correction D3 (referred to as B3LYP-D3) [20]) unless explicitly stated otherwise. Geometries were optimized with the triple-ζ basis set 6-311G(d,p) (referred to as BS1), including the IEFPCM solvent model (CH_3CN) [21]. Thermochemical quantities were obtained from frequency calculations at the same level of theory as optimizations, with the temperature set to 298 K. Single point calculations with 6-311++G(2df,2p) (referred to as BS2) were performed to obtain more accurate electronic energies, and the free energies were corrected accordingly. Standard state (SS) conversions were performed to convert the energies from a 1 atm standard state to a 1 M solution standard state, which amount to +1.89 kcal/mol at 298 K for dissociative reaction steps. Counterpoise (CP) corrections were computed for HCl to correct for the basis set super position error upon removal of HCl from the model (from Inter3). The final free energies are thus computed as: $G_{BS2} = G_{BS1} - E_{BS1} + E_{BS2} + SS + CP_{BS2}$. Optimized coordinates are given in the Supporting Information.

2.5 X-ray crystal structure determination

Data for complexes **2** and **4** were collected at 150 K on a Bruker D8 Venture kappa geometry diffractometer, with duo Iμs sources, a Photon 100 CMOS detector and APEX II control software using Quazar multi-layer optics, monochromated Mo-Kα radiation and by means of a combination of ϕ and ω scans. Data reduction was performed using SAINT+ and the intensities were corrected for

absorption using SADABS [22]. The structures were solved by intrinsic phasing using SHELXTS and refined by full-matrix least squares using SHELXTL and SHELXL-2013 [23]. In the structure refinement, all hydrogen atoms were added in calculated positions and treated as riding on the atom to which they are attached. All nonhydrogen atoms were refined with anisotropic displacement parameters, all isotropic displacement parameters for hydrogen atoms were calculated as X × Ueq of the atom to which they are attached, X = 1.5 for the methyl hydrogens and 1.2 for all other hydrogens. Crystallographic data and refinement parameters are given in Table 3 and Table 5. Ortep drawings [24] of the structures are included in Figure 7 and Figure 9. The crystal structures (cif) have been deposited at the Cambridge Crystallographic Data Centre and allocated the deposition numbers: CCDC 1478542-1478543. Data collection, structure solution and refinement details are available in each cif.

3 Results and Discussion

3.1 Synthesis of $[Ti(tfba)_2Cl_2]$ (1) and $[Ti(tfba)_2biphen]$ (2)

$[Ti(tfba)_2Cl_2]$ is synthesized from $TiCl_4$, substituting two chloro-ligands with two trifluorobenzoylacetonato ($tfba^-$) ligands in dichloromethane. Substituting the remaining two chloro-ligands in $[Ti(tfba)_2Cl_2]$ with the bidentate ligand $biphen^{2-}$, leads to $[Ti(tfba)_2biphen]$, see Scheme 1. The hydrolytic stability of $[Ti(tfba)_2Cl_2]$ relative to $[Ti(acac)_2Cl_2]$ was tested in acetonitrile. When 5 mMol complex was dissolved in dry CH_3CN treated with 6.25 % water, TiO_2 precipitates within 20 s and 60 s respectively. $[Ti(tfba)_2biphen]$, when treated under similar conditions, exhibits enhanced water stability and did not precipitate within 6 weeks [15].

For a drug to be tested in preclinical toxicological and pharmacological studies it needs to be relatively insensitive to hydrolysis to prevent problems with the galenic formulation [25]. Thus the hydrolytic stability of $[Ti(tfba)_2biphen]$ makes it suitable for medical testing, compared to the hydrolytically unstable $[Ti(tfba)_2Cl_2]$.

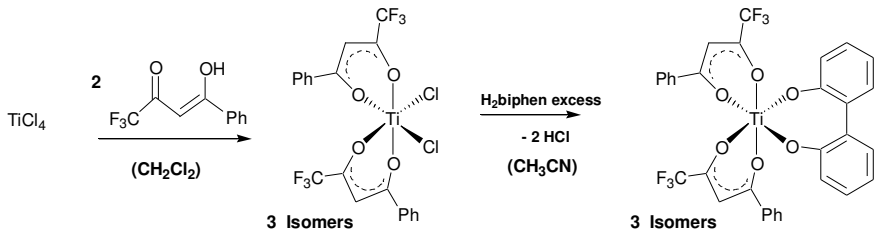

Scheme 1. Synthesis of [Ti(tfba)$_2$Cl$_2$] (1) and [Ti(tfba)$_2$biphen] (2) from TiCl$_4$.

While five isomers (two *trans* and three *cis*) are possible for [Ti(tfba)$_2$Cl$_2$], (**1**), only the three *cis* isomers are possible for [Ti(tfba)$_2$biphen], (**2**), see Figure 2. Theoretical calculations utilizing force field [26,27] and density functional theory [15], as well as experimental studies [26,28,29,30,31] showed that *trans* [Ti(β-diketonato)$_2$X$_2$] isomers for X = F, Cl, Br, OR, are unlikely and that only when X is the more bulky iodo ligand, are *trans* isomers possible [32] and indeed observed [33]. The existence of the three *cis* isomers of (**1**) and (**2**) can only be observed on low temperature NMR, since at very low temperatures the interconversion between the individual isomers is slow and the ^{1}H NMR spectrum consists of sharp peaks arising from the protons in the three different isomers. As the temperature is increased, the rate of interconversion between the isomers becomes faster than the NMR time scale and the peaks first broaden and then merge into a single broad peak (at RT) and finally at 55°C, give rise to a narrow peak at the average position of each type of proton, see the spectra obtained at different temperatures in Figure 4 (a).

Four peaks corresponding to the resonance of the methine proton (CH) of the β-diketonato ligand and also four sets of peaks corresponding to the resonance of the protons of the phenyl groups are expected for the three *cis* isomers of [Ti(tfba)$_2$Cl$_2$]. Isomers, *cis-trans-cis* and *cis-cis-trans*, both have one peak for the resonance of the methine H and one set of peaks for the resonance of the phenyl protons due to their C_2 symmetry. The *cis-cis-cis* isomer, due to its low symmetry, has two peaks of equal intensity for the methine H resonance and two sets of peaks of equal intensity for the phenyl protons resonance on ^{1}H NMR. The isomer distribution obtained from low temperature NMR is 37:38:25 and 17:62:21 for *cis-cis-cis*:*cis-cis-trans*:*cis-trans-cis* for [Ti(tfba)$_2$Cl$_2$] and [Ti(tfba)$_2$biphen] respectively [15], see Figure 2 for the naming of the isomers.

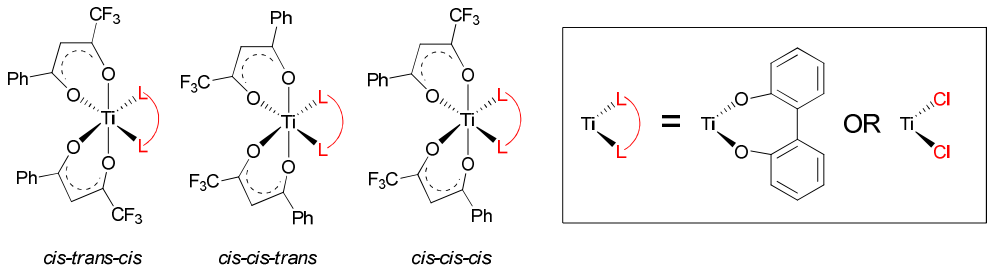

Figure 2. ***Cis*** **geometric-isomers of octahedral [Ti(tfba)$_2$Cl$_2$] and [Ti(tfba)$_2$biphen] complexes. The** ***cis*** **isomers are named by referring to 1. LL, 2. CF$_3$ and 3. Ph. The** ***trans*** **isomers of [Ti(tfba)$_2$Cl$_2$] were not observed.**

As described below in section 3.4, only the *cis-cis-trans* and *cis-trans-cis* isomers of [Ti(tfba)$_2$biphen] were isolated in the solid state. This result could be interpreted in terms of a difference in [Ti(tfba)$_2$Cl$_2$] isomers reactivity, however, NMR shows that the three possible isomers of [Ti(tfba)$_2$biphen] are in fast equilibrium and are all present in solution, Figure 3. The observation of only two isomers in the X-ray crystal structure is therefore assumed to be due to preferential crystallization and does not provide information about differences in reactivity of the different [Ti(tfba)$_2$Cl$_2$] isomers. If substitution of one [Ti(tfba)$_2$Cl$_2$] isomer is preferred, the equilibrium between the three [Ti(tfba)$_2$Cl$_2$] isomers will be re-instated till completion of the substitution reaction. The same applies for the product isomers.

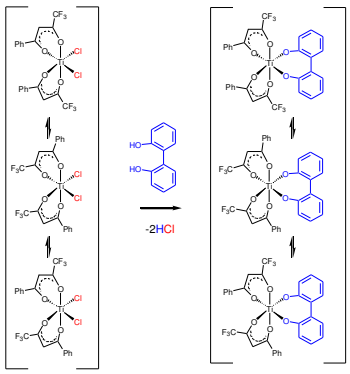

Figure 3. Three *cis* geometric-isomers of [Ti(tfba)$_2$Cl$_2$] in fast equilibrium with each other form the three *cis* geometric-isomers of [Ti(tfba)$_2$biphen], also in fast equilibrium with each other, during the [Ti(tfba)$_2$Cl$_2$] + H$_2$biphen substitution reaction.

3.2 Hydrolysis of [Ti(tfba)$_2$Cl$_2$]

In $CDCl_3$ solution, it was previously shown that [Ti(β-diketonato)$_2$Cl$_2$] complexes with CF_3-containing β-diketonato ligands $(CF_3COCHCOR)^-$ with R = CF_3, C_4H_3S, C_4H_3O, CH_3 [16], CH_2CH_3, $CH(CH_3)_2$ or $C(CH_3)_3$ [32], exist in equilibrium with a hydrolysed dinuclear [{Ti(β-diketonato)$_2$Cl}$_2$(μ-O)] complex in $CDCl_3$ containing trace amounts of water. The equilibrium reaction is

$$2\ [\text{Ti}(\beta\text{-diketonato})_2\text{Cl}_2] + H_2O \rightleftharpoons [\{\text{Ti}(\beta\text{-diketonato})_2\text{Cl}\}_2(\mu\text{-O})] + 2HCl.$$

This same equilibrium reaction was observed for the CF_3-containing complex [Ti(tfba)$_2$Cl$_2$] of this study. The ^{1}H NMR of [Ti(tfba)$_2$Cl$_2$] at 55°C, 21°C, and -60°C is shown in Figure 4 (a). At 21°C the peaks are broad due to the relatively fast equilibrium between the three *cis* isomers. Upon heating (55°C), two set of peaks are clearly observed with the doublets and triplets of the phenyl protons clearly defined. The one set of peaks corresponds to the resonance of the protons of the three *cis* isomers of [Ti(tfba)$_2$Cl$_2$] and the second set of peaks to the resonance of the protons of the ten hydrolysed dinuclear [{Ti(tfba)$_2$Cl}$_2$(μ-O)] isomers. The structures of the ten possible dimeric isomers of [{Ti(tfba)$_2$Cl}$_2$(μ-O)] are given in Figure S1 of the Supporting Information. At low temperature (-60°C) the interchange between the three [Ti(tfba)$_2$Cl$_2$] isomers and also between the ten [{Ti(tfba)$_2$Cl}$_2$(μ-O)] isomers is slower and separate peaks for most of the isomers can be identified on ^{19}F NMR. For example, four separated sharp peaks between -73.5 and -74.5 ppm, corresponding to the resonance of the CF_3 groups of the three *cis* [Ti(tfba)$_2$Cl$_2$] isomers, and between 20 and 30 peaks, corresponding to the resonance of the CF_3 groups of the ten [{Ti(tfba)$_2$Cl}$_2$(μ-O)] isomers, are clearly observed, see Figure 4 (b). Similarly on the ^{1}H NMR spectra, the one sharp peak, 7.03 ppm, (50°C) slits into the four peaks (-60°C) corresponding to the three *cis* [Ti(tfba)$_2$Cl$_2$] isomers and the upfield

peak at 6.02 ppm (50°C) splits into multiple peaks of the expected maximum 32 peaks (-60°C), corresponding to the ten [{Ti(tfba)$_2$Cl}$_2$(μ-O)] isomers. The formation of the dinuclear complex [{Ti(tfba)$_2$Cl}$_2$(μ-O)] from [Ti(tfba)$_2$Cl$_2$], made possible due to trace amounts of water present in the $CDCl_3$, leads to a dynamic equilibrium between the three *cis* isomers of [Ti(tfba)$_2$Cl$_2$] and the ten hydrolysed dinuclear [{Ti(tfba)$_2$Cl}$_2$(μ-O)] isomers. With a slight increase in trace amounts of water, monomeric [Ti(tfba)$_2$Cl$_2$] is converted to tetranuclear [Ti(tfba)$_2$(μ-O)]$_4$, according to

$$4\ [Ti(tfba)_2Cl_2] + 4\ H_2O \rightarrow [Ti(tfba)_2(\mu\text{-}O)]_4 + 8HCl.$$

[Ti(tfba)$_2$(μ-O)]$_4$ is not involved in any equilibrium in $CDCl_3$ solution, see the ^{1}H NMR in Figure 4 (c). The crystal structure of [Ti(tfba)$_2$(μ-O)]$_4$, presented in Section 3.5, has a S_4 molecular symmetry, see Figure 10, and therefore only one signal for the resonance of the methine proton, and one set of signals for the phenyl protons, were observed on ^{1}H NMR. However, with an excess of water, decomposition of [Ti(tfba)$_2$Cl$_2$] to TiO_2 takes place, visually observed by the formation of a fine white powder. Figure 5 give a summary of the reactions discussed in which [Ti(tfba)$_2$Cl$_2$] is involved.

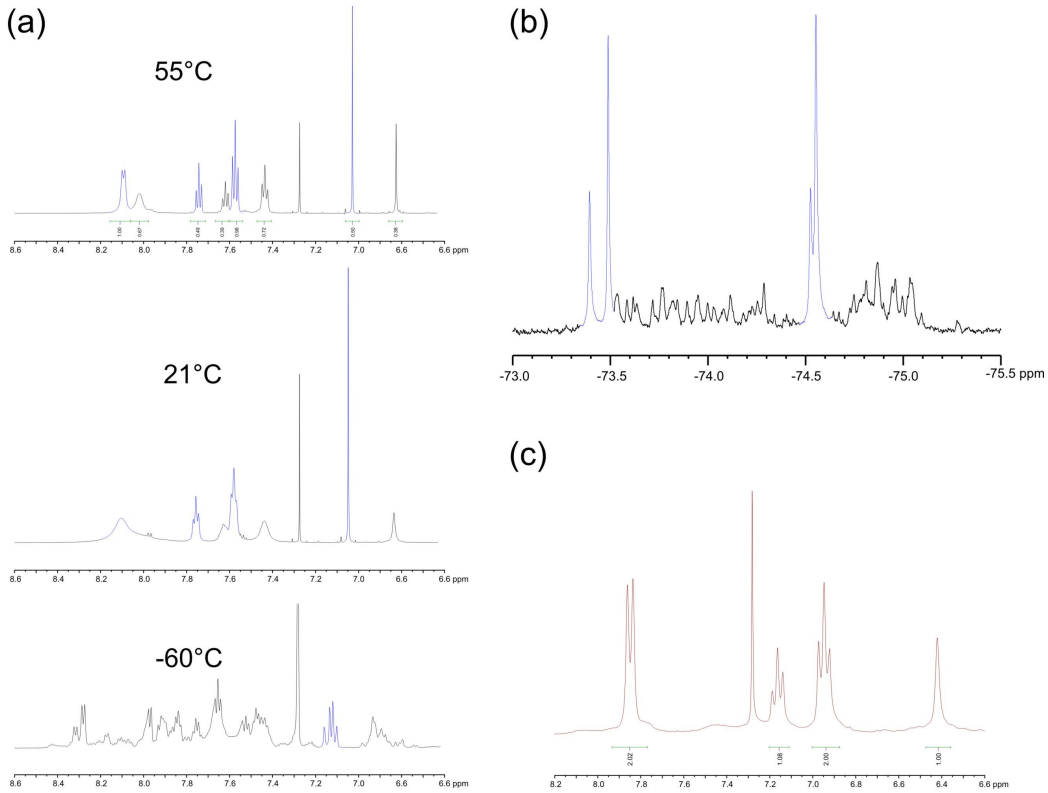

Figure 4. (a) ^{1}H NMR at different temperatures and (b) ^{19}F NMR at -60 °C of the equilibrium reaction between mononuclear [Ti(tfba)$_2$Cl$_2$] (resonance of the methine proton (CH) of the β-diketonato ligand and selected other

resonances shown in blue) and dinuclear [Ti(tfba)$_2$Cl}(μ-O)] in CDCl$_3$ containing trace amounts of water and acid. (c) ^{1}H NMR at 21°C of tetranuclear [Ti(tfba)$_2$(μ-O)]$_4$.

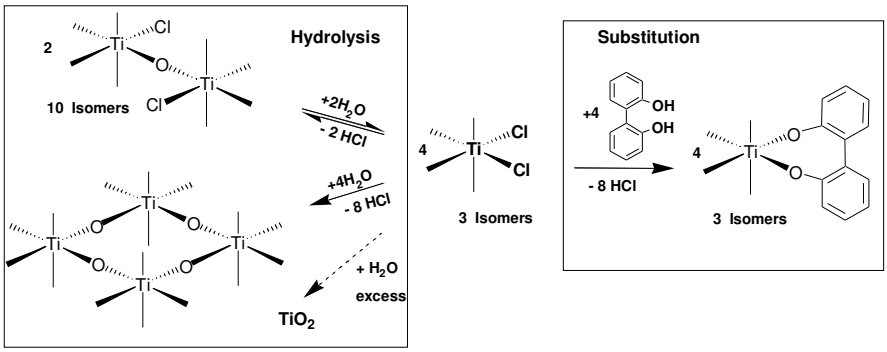

Figure 5. Schematic presentation of the reaction of [Ti(tfba)$_2$Cl$_2$] with water or with [1,1'-Biphenyl]-2,2'-diol. For simplification, the β-diketonato backbone is omitted.

The chemical shifts of the methine proton of the tfba-ligand in the coordinate complexes (**1**) – (**4**) and for the uncoordinated Htfba (included for comparison) are listed in Table 1. The resonance of the methine proton of the chelated complexes (**1**) – (**3**) is slightly downfield shifted relative to the uncoordinated ligand. Comparing shifts of the resonance of the methine proton, the mononuclear complex [Ti(tfba)$_2$Cl$_2$] (δ = 7.05 ppm) (**1**), the dinuclear complex [{Ti(tfba)$_2$Cl}$_2$(μ-O)] (δ = 6.89 ppm) (**3**) and the tetranuclear complex [Ti(tfba)$_2$(μ-O)]$_4$ (δ = 6.85 ppm) (**4**), we observe that the resonance of the methine proton gradually shifts upfield as the chloro ligands are substituted by more electron donating oxygens. The resonance of the methine proton of [Ti(tfba)$_2$(biphen)] (**2**) (δ = 6.98 ppm) is slightly upfield shifted relative to the parent complex [Ti(tfba)$_2$Cl$_2$] (δ = 7.05 ppm) (**1**) as expected since the chloro ligand is more electron-withdrawing than the biphen ligand.

Table 1. ^{1}H NMR chemical shifts for the methine protons of complexes **1** - **4**.

No	Compound	^{1}H / ppm methine H
-	Htfba	6.59
1	[Ti(tfba)$_2$Cl$_2$]	7.05
2	[Ti(tfba)$_2$biphen]	6.89

3	$[Ti(tfba)_2Cl\}_2(\mu\text{-}O)]$	6.85
4	$[Ti(tfba)_2(\mu\text{-}O)]_4$	6.42

3.3 Substitution kinetics of $[Ti(tfba)_2Cl_2]$

The substitution reaction $[Ti(tfba)_2Cl_2]$ + H_2biphen was followed on the UV/vis at 450 nm in CH_3CN. Two reaction steps were observed, the first relatively fast reaction step that was [H_2biphen] dependent, and a second slower step that was [H_2biphen] independent. The first step of the substitution reaction was first-order kinetics with [H_2biphen] in excess. The kinetic results thus showed simple second order kinetics with a non-zero intercept. The results are given in Figure 6 and Table 2.

In CH_3CN, $[Ti(acac)_2Cl_2]$ exist as $[Ti(acac)_2Cl_2]$, as well as a solvent coordinated species, proposed to be $[Ti(acac)_2Cl_2(CH_3CN)]$, in a ratio of 10:1 as observed in ^{1}H NMR [36]. We here propose a similar equilibrium between $[Ti(tfba)_2Cl_2]$ and $[Ti(tfba)_2Cl_2(CH_3CN)]$, to explain the non-zero intercept. The $[Ti(tfba)_2Cl_2]$ + H_2biphen reaction can thus follow a direct and a solvent pathway, see Scheme 2.

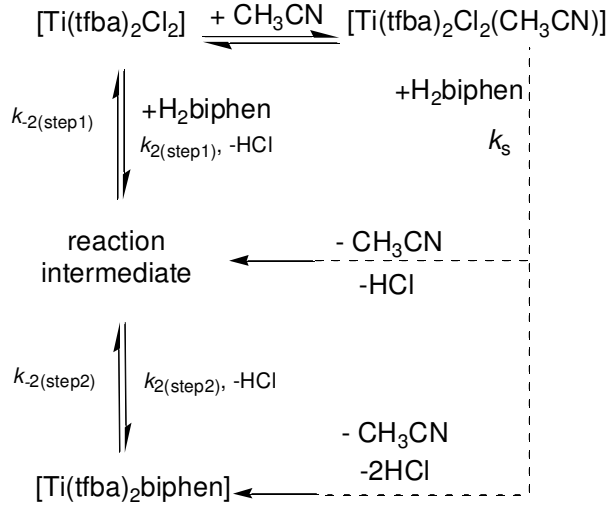

Scheme 2: Proposed scheme for the $[Ti(tfba)_2Cl_2]$ + H_2biphen substitution reaction in CH_3CN, that involves a direct and a solvent pathway.

The negative activation entropy value obtained indicates either an associative or interchange mechanism. An associative mechanism implies the formation of a 7-coordinated activated complex, followed by a 7-coordinated intermediate while an interchange mechanism implies the formation of a 7-coordinated activated complex, followed by a 6-coordinated intermediate. Since a stable 6-coordinated intermediate, $[Ti(acac)_2(Cl)(Hnaph)]$, of a related reaction, $[Ti(acac)_2Cl_2]$ + H_2naph (H_2naph = 2,3-dihydroxynaphthalene or naphthol), was isolated [34], the experimental results are consistent with the first step being the substitution of the first Cl^- leading to the 6-coordinated intermediate $[Ti(tfba)_2(Cl)(Hbiphen)]$, and the second step the substitution of the second Cl^- to form the product $[Ti(tfba)_2biphen]$, in agreement with related reactions [35,36].

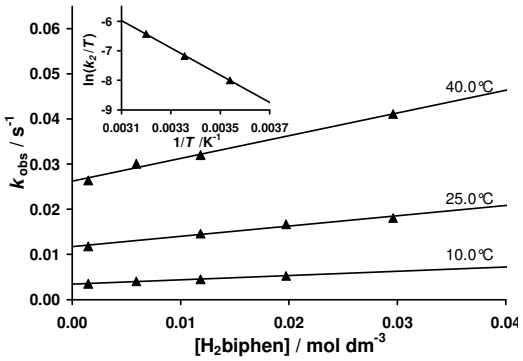

Figure 6. Graph of the observed pseudo first order rate constant k_{obs} *vs* H_2biphen concentration for the $[Ti(tfba)_2Cl_2]$ + H_2biphen substitution reaction in CH_3CN. $[Ti(tfba)_2Cl_2]$ = 0.1 mmol dm^{-3}. Inset: Linear dependence between $\ln(k_{2\ (step\ 1)}/T)$ and $1/T$, as predicted by the Eyring equation ($k_{2\ (step\ 1)}$ is the second order rate constant of the first reactions step, obtained from the slope of the k_{obs} *vs* [H_2biphen] graph).

Table 2. Kinetic data and activation parameters for the first step of the substitution reaction of biphen^{-2} for the monodentate Cl^- ligands from $[Ti(tfba)_2Cl_2]$ in CH_3CN as solvent according to Scheme 2.

T / °C	$k_{2\ (step\ 1)}$ / $dm^3mol^{-1}s^{-1}$	$k_{S\ (step\ 1)}$ / s^{-1}	$\Delta H^{\ddagger}$ / kJ mol^{-1}	$\Delta S^{\ddagger}$ / J mol^{-1} K^{-1}	$\Delta G^{\ddagger}$ / kJ mol^{-1}
15.0	0.062	0.0001			
25.0	0.153	0.0046	59.6	-62	78

36.2	0.365	0.0133

3.4 Crystal structure of [Ti(tfba$_2$)biphen] (2)

Complex (**2**) was crystallized from a DCM:hexane (1:1) solution as red-black cubic-shaped crystals. Both the *cis-cis-trans* and *cis-trans-cis* isomers of [Ti(tfba)$_2$biphen] were present, in a 2:1 ratio, in the unit cell of (**2**). Two molecules of the *cis-cis-trans* isomer and two half molecules of the *cis-trans-cis* isomer (both these Ti atoms, Ti(3) and Ti(4), occur on 2-fold axes that generate the full molecules), result in a total of three molecules per asymmetric unit. The observed isomer distribution of [Ti(tfba)$_2$biphen] in $CDCl_3$ solution quantitatively agrees with the 2:1 ratio: *cis-cis-trans* (62%) and *cis-trans-cis* (21%) and *cis-cis-cis* (17%). The *cis-cis-trans* and *cis-trans-cis* isomers of [Ti(tfba)$_2$biphen] exhibit C_2 molecular symmetry, see Figure 8. The two types of molecules of the unit cell are shown in **Figure 7** and the remaining molecule in The Electronic Supporting Information. The molecule containing Ti(2) resembles the isomeric structure of that containing Ti(1), while the molecule containing Ti(4) exhibits the *cis-trans-cis* isomer, similar to the molecule containing Ti(3).

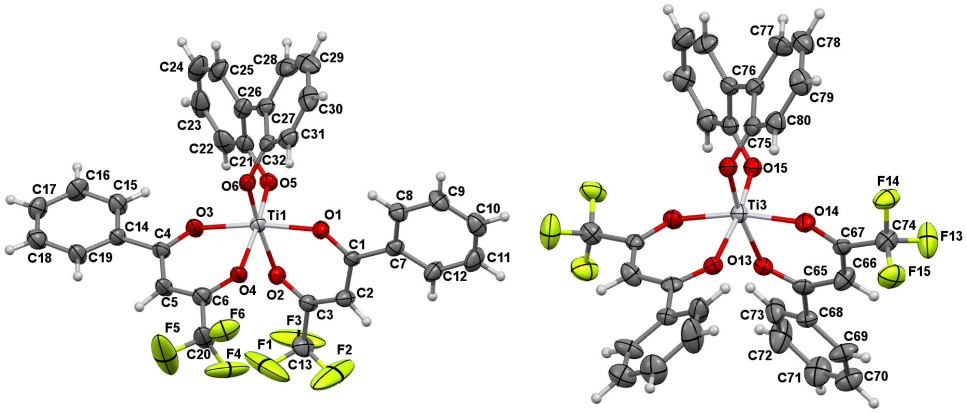

Figure 7. Two isomeric molecular structures (50% probability displacement ellipsoids) of [Ti(tfba$_2$)biphen)] (2) showing the numbering scheme.

The Ti-O bond lengths range from 1.816(5) Å for Ti(2)-O(12) to 2.039(5) Å for Ti(2)-O(8). Two factors seem to influence the Ti-O bond lengths: (i) the identity of the closest substituent of the β-diketonato moiety to the specific Ti-O bond, phenyl or CF_3; and (ii) the *trans* ligand environment, i.e. whether the Ti-O bond is *trans* to a Ti-O bond with a closer phenyl-substituted β-diketonato ligand, a closer CF_3-substituted β-diketonato ligand or a biphenyl group. For the *cis-cis-trans* isomers (Ti(1)- and Ti(2)-containing molecules) the following trend is observed for the Ti-O bond lengths: biphenyl (1.824(5) Å average) < phenyl (2.003(5) Å average) < CF_3 (2.033(5) Å average). For the *cis-trans-cis* isomers (Ti(3)- and Ti(4)-containing molecules) this trend changes to biphenyl (1.833(5) Å average) < CF_3 (1.998(5) Å average) < phenyl (2.030(5) Å average). In each molecule, the two Ti-O bonds associated with biphen are always the shortest and the Ti-O bonds *trans* to these two bonds are always the longest. The O-C bond lengths show an inverse trend. For all four molecules the O-C_{biphen} bonds are longer (1.351(8) Å average) than the O-C_{Ph} (1.269(8) Å average) and O-C_{CF3} (1.275(8) Å average) bonds, which are approximately equal. Two slightly different sets of C-C bonds lend an asymmetry to the β-diketonato ligand. The side with the CF_3 substituent shows a shorter C-C bond (1.364(10) Å average) than the side containing a phenyl substituent (1.406(10) Å average). Due to this asymmetry in bond lengths, the related bond angles are affected, with average value of the bond angle around the carbon atom bearing the CF_3 substituent is approximately 6° larger that the corresponding angle for the carbon atom containing the phenyl substituent. There is significant rotational disorder associated with most of the CF_3 groups. However, it is of importance to note that C-F bond lengths vary from 1.262(11) Å on average (C(13)F_3) to 1.333(9) Å on average (C(74)F_3) with the *cis-trans-cis* isomers displaying longer C-F bond lengths in general, compared to the *cis-cis-trans* isomers. O-Ti-O_{cis} bond angles ranges from 82.0(2)° to 100.2(2)° while O-Ti-O_{trans} bond angles vary between 168.2(3)° and 172.1(2)°. From the torsion angles determined, it is clear that the β-diketonato ligands are all close to planarity, with the two *cis-trans-cis* isomers showing the smallest deviation from planarity (0.8° average) compared to the two *cis-cis-trans* isomers (9.4° average). The torsion angle between the two phenyl rings of the biphenyl moiety is 44.1° on average, with all four molecules having similar values.

Table 3. Selected geometric parameters for 2

Bond length (Å)			
Ti(1)-O(1)	2.004(5)	O(1)-C(1)	1.281(8)
Ti(1)-O(2)	2.033(5)	O(2)-C(3)	1.267(8)
Ti(1)-O(3)	2.005(5)	O(3)-C(4)	1.251(8)
Ti(1)-O(4)	2.033(5)	O(4)-C(6)	1.276(9)
Ti(1)-O(5)	1.828(5)	O(5)-C(21)	1.368(8)
Ti(1)-O(6)	1.825(5)	O(6)-C(32)	1.345(8)
Ti(2)-O(7)	2.014(5)	O(7)-C(33)	1.266(8)
Ti(2)-O(8)	2.039(5)	O(8)-C(35)	1.267(8)
Ti(2)-O(9)	1.990(5)	O(9)-C(36)	1.278(8)
Ti(2)-O(10)	2.028(5)	O(10)-C(38)	1.275(8)
Ti(2)-O(11)	1.828(5)	O(11)-C(53)	1.356(8)
Ti(2)-O(12)	1.816(5)	O(12)-C(64)	1.357(8)
Ti(3)-O(13)	2.036(5)	O(13)-C(65)	1.268(8)
Ti(3)-O(14)	1.995(5)	O(14)-C(67)	1.287(8)
Ti(3)-O(15)	1.831(5)	O(15)-C(75)	1.342(9)
Ti(4)-O(16)	2.023(5)	O(16)-C(81)	1.286(8)
Ti(4)-O(17)	2.001(5)	O(17)-C(83)	1.276(8)
Ti(4)-O(18)	1.834(5)	O(18)-C(91)	1.347(9)
C(1)-C(2)	1.419(10)	C(36)-C(37)	1.400(10)
C(2)-C(3)	1.365(10)	C(37)-C(38)	1.360(10)
C(4)-C(5)	1.393(10)	C(65)-C(66)	1.413(10)
C(5)-C(6)	1.381(10)	C(66)-C(67)	1.370(10)
C(33)-C(34)	1.417(9)	C(81)-C(82)	1.396(10)
C(34)-C(35)	1.354(10)	C(82)-C(83)	1.354(10)
Bond angles (°)			
O-Ti-O_{cis}	89.7(2) av	O-Ti-O_{trans}	170.7(2) av
O-C(CF_3)[a]-C(β)[b]	127.5(7) av	O-C(Ph)[a]-C(β)[b]	121.5(6) av

Torsion angles (°)			
O- $C(CF_3)^a$-$C(Ph)^a$-O for Ti(1)	10.1 av[c]	C(21)-C(26)-C(27)-C(32)	-43.3(11)
O- $C(CF_3)^a$-$C(Ph)^a$-O for Ti(2)	-8.7 av	C(53)-C(58)-C(59)-C(64)	44.4(11)
O- $C(CF_3)^a$-$C(Ph)^a$-O for Ti(3)	0.5 av	C(75)-C(76)-C(76)#-C(75)#	-45.0
O- $C(CF_3)^a$-$C(Ph)^a$-O for Ti(4)	0.1 av	C(91)-C(92)-C(92)#-C(91)#	43.5

[a] Carbon atom of β-diketonato ligand containing substituent

[b] Central carbon atom of β-diketonato ligand

[c] Values without standard deviation were measured in Mercury

There are noticeable differences in the dihedral angles (C2-C1-C1'-C2') of the 2,2'-biphenyl moieties of the 3,3'5,5'-tetrasubstituted biphenyl-2,2'-diolato complexes, where R = R3 = R3' = R5 = R5' (Table 4). The smallest dihedral angles are generally associated with least bulky substituents, H-atoms, in the 3,3',5,5' positions. The largest dihedral angles result from more steric interactions of the more bulky NO_2 groups in the 5,5' positions, while the interactions between the smaller CH_3-groups in the 5,5'-postions results in a reduction in the biphenyl dihedral angles.

Table 4. Biphenyl dihedral angles (C2-C1-C1'-C2') in selected literature compounds

Substituent R	**Biphenyl dihedral angle (°)**	**Reference**	**CCDC Refcode**
H	44.1 (av)	Complex **2**	
H	46.9	15	XUGHEN
H	47.9	36	MOMXOC
CH_3	50.8	37	OJOBIZ
CH_3	47.0	37	OJOBOF
NO_2	54.7	37	OJOBUL

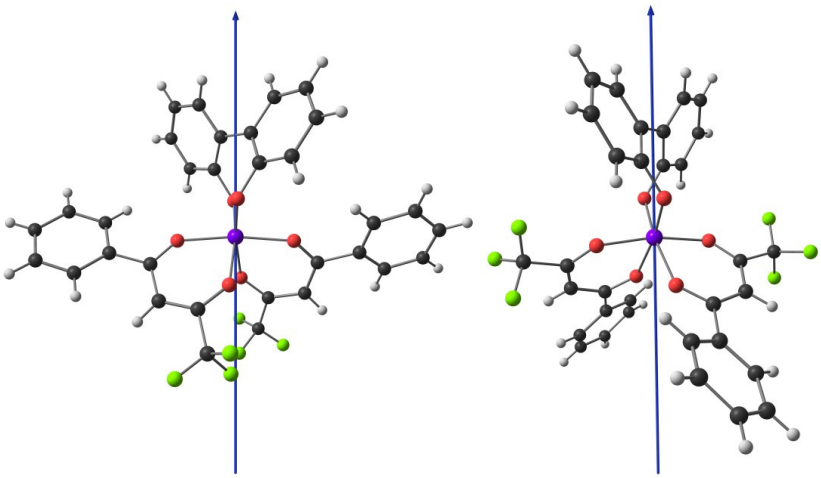

(a) (b)

Figure 8. The structure of (a) *cis-cis-trans* and (b) *cis-trans-cis* [Ti(tfba$_2$)biphen)] (2), illustrating the C_2 molecular symmetry with the C_2 axis shown in blue. Color code of atome (online version): Ti (purple), O (red), C (dark grey), F (green) and H (white).

3.5 Crystal structure of tetranuclear complex (4)

The tetranuclear complex (**4**) was crystallized from a DCM:hexane (1:1) solution as yellow-green block-shaped crystals and comprises of four *cis-cis-trans* [Ti(tfba)$_2$Cl$_2$] isomer moieties. The eight β-diketonato backbones and the four bridging oxygens have a S_4 molecular symmetry, see Figure 10. In $CDCl_3$ solution the observed isomer distribution of [Ti(tfba)$_2$Cl$_2$] was *cis-cis-trans* (38%) and *cis-trans-cis* (25%) and *cis-cis-cis* (37%).

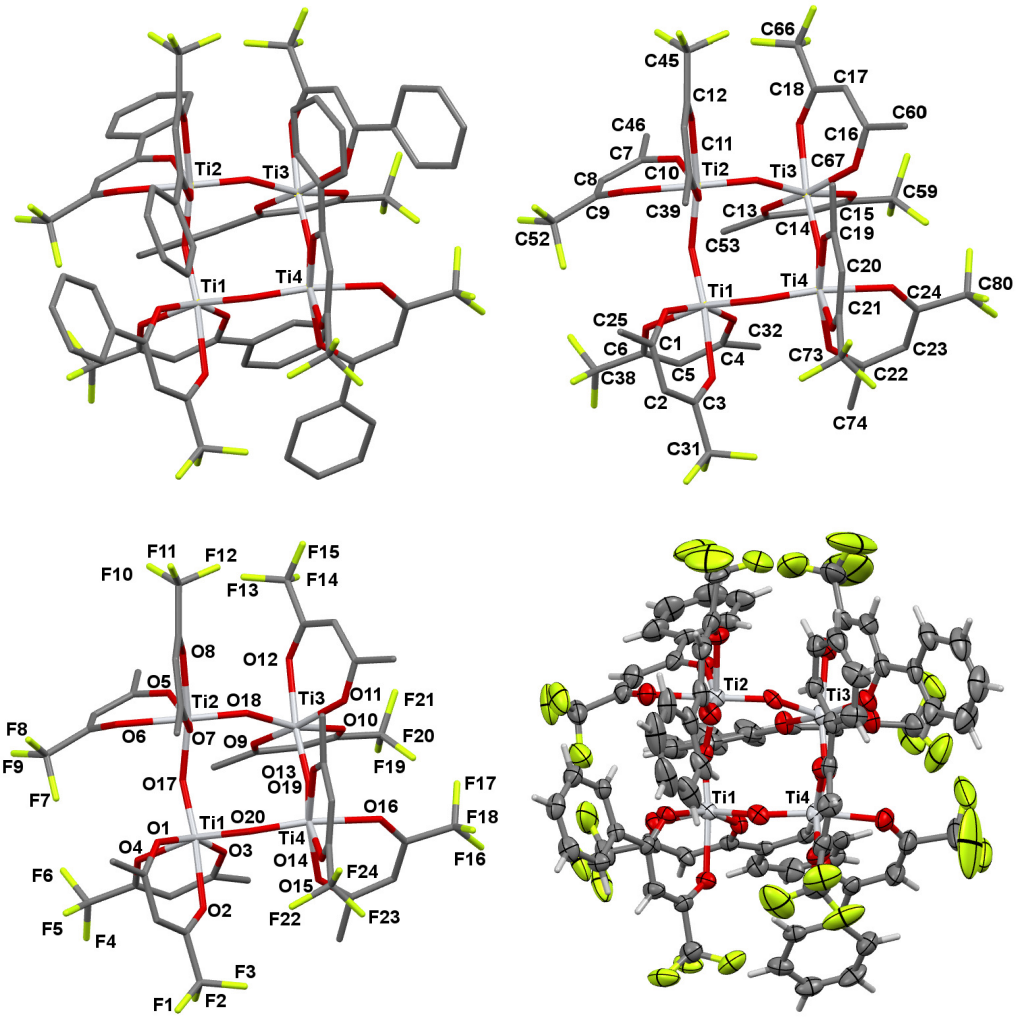

Figure 9. The molecular structure (Stick models to show the numbering scheme and as well as the ellipsoid structure with 50 % probability displacement ellipsoids) of tetranuclear complex $[Ti(tfba)_2(\mu\text{-}O)]_4$ (4). Hydrogens and selected phenyl rings were omitted for clarity.

The Ti-O bond lengths range from 1.750(3) Å for Ti(1)-O(17) to 2.133(3) Å for T(1)-O(2). Three different bond length ranges can be distinguished, depending on the environment of the specific Ti-O bond. The first two groups of bond lengths seem to differ depending on the terminal group on the carbon atom of β-diketonato moiety adjacent to the specific Ti-O bond, in this case a phenyl group (1.946(3)-1.989(3) Å) or a CF_3 group (2.050(3)-2.133(3) Å) while the third group is associated with the bridging Ti-O-Ti moiety (1.750(3)-1.878(3) Å). Therefore the trend for Ti-O bond lengths seems to be: bridging O group < phenyl < CF_3. This observation correlates with similar trends for the *cis-cis-*

trans isomers of (**2**). For the β-diketonato carbon backbone, the C-C bond for the part associated with the phenyl substituent is in general slightly longer (1.395(7) Å average) than the C-C bond associated with the CF_3 substituent (1.372(7) Å average). Both bonds exhibit double bond character, as expected for a β-diketonato ligand. This same trend is observed for the O-C bonds of the β-diketonato ligand phenyl-substituted side (1.279(6) Å average) compared to the CF_3-substituted side (1.261(6) Å average). C-F bond lengths again vary quite a bit due to rotational disorder in the molecule (1.246(13)-1.336(7) Å). O-Ti-O_{cis} bond angles differ from 80.76(12) Å to 101.13(15) Å while O-Ti-O_{trans} bond angles range between 159.06(14) Å and 177.13(13) Å. Torsion angles for all the β-diketonato ligands (O-C(CF_3)-C(Ph)-O) indicate near-planarity, with the largest deviation by the β-diketonato ligands of the Ti(2) moiety (8.4° average). Ti-Ti-Ti bond angles have similar values for opposite angles with an average value of 84.0° for the four angles. The four metal atoms do not lie in the same plane as a dihedral angle (Ti(1)-Ti(2)-Ti(3)-Ti(4)) of -35.7° indicates.

Table 5. Selected geometric parameters for 4

Bond length (Å)			
Ti(1)-O(1)	1.982(3)	Ti(1)-O(17)	1.750(3)
Ti(1)-O(2)	2.133(3)	Ti(1)-O(20)	1.849(3)
Ti(1)-O(3)	1.989(3)	Ti(2)-O(17)	1.878(3)
Ti(1)-O(4)	2.050(3)	Ti(2)-O(18)	1.752(3)
Ti(2)-O(5)	1.946(3)	Ti(3)-O(18)	1.875(3)
Ti(2)-O(6)	2.123(3)	Ti(3)-O(19)	1.770(3)
Ti(2)-O(7)	1.968(3)	Ti(4)-O(19)	1.861(3)
Ti(2)-O(8)	2.060(4)	Ti(4)-O(20)	1.760(3)
Ti(3)-O(9)	1.971(3)	Ti(4)-O(13)	1.982(3)
Ti(3)-O(10)	2.058(4)	Ti(4)-O(14)	2.077(3)
Ti(3)-O(11)	1.963(3)	Ti(4)-O(15)	1.986(3)
Ti(3)-O(12)	2.112(4)	Ti(4)-O(16)	2.115(3)

C(1)-C(2)	1.402(6)	O(1)-C(1)	1.273(5)
C(2)-C(3)	1.376(7)	O(2)-C(3)	1.250(5)
C(4)-C(5)	1.410(6)	O(3)-C(4)	1.275(5)
C(5)-C(6)	1.382(6)	O(4)-C(6)	1.259(5)
C(7)-C(8)	1.382(7)	O(5)-C(7)	1.284(5)
C(8)-C(9)	1.376(7)	O(6)-C(9)	1.269(6)
C(10)-C(11)	1.387(8)	O(7)-C(10)	1.295(6)
C(11)-C(12)	1.359(8)	O(8)-C(12)	1.262(6)
C(13)-C(14)	1.408(7)	O(9)-C(13)	1.265(5)
C(14)-C(15)	1.364(7)	O(10)-C(15)	1.272(6)
C(16)-C(17)	1.384(8)	O(11)-C(16)	1.283(6)
C(17)-C(18)	1.381(8)	O(12)-C(18)	1.250(6)
C(19)-C(20)	1.408(7)	O(13)-C(19)	1.276(5)
C(20)-C(21)	1.365(7)	O(14)-C(21)	1.263(6)
C(22)-C(23)	1.377(7)	O(15)-C(22)	1.280(5)
C(23)-C(24)	1.374(8)	O(16)-C(24)	1.264(6)
Bond angle (°)			
O-Ti-O_{cis}	89.02(13) av	O-Ti-O_{trans}	167.98(13) av
O-C(CF_3)[a]-C(β)[b]	127.8(5) av	O-C(Ph)[a]-C(β)[b]	121.7(4) av
Ti(1)-Ti(2)-Ti(3)	82.1[c]	Ti(3)-Ti(4)-Ti(1)	83.3
Ti(2)-Ti(3)-Ti(4)	85.5	Ti(4)-Ti(1)-Ti(2)	85.1
Torsion angle (°)			
O-C(CF_3)[a]-C(Ph)[a]-O for Ti(1)	2.3 av	O-C(CF_3)[a]-C(Ph)[a]-O for Ti(3)	2.2 av
O-C(CF_3)[a]-C(Ph)[a]-O for Ti(2)	8.4 av	O-C(CF_3)[a]-C(Ph)[a]-O for Ti(4)	3.1 av
Ti(1)-Ti(2)-Ti(3)-Ti(4)	-35.7		

[a] Carbon atom of β-diketonato ligand containing substituent

[b] Central carbon atom of β-diketonato ligand

[c] Values without standard deviation were measured in Mercury

The planarity of the β-diketonato ligand, as measured by the O-C(R1)-C(R2)-O dihedral angle where R1 and R2 are the substituents on the β-diketonato ligand, $(R1COCHCOR2)^-$, showed little change with variations of R1 and R2 in related multinuclear Ti complexes containing β-diketonato ligands (Table 6). However, the $(Ti\text{-}O)_4$-ring in **4,** with R1 = CF_3 and R2 = Ph as substituents on the β-diketonato ligand is non-planar. This cyclic system is severely puckered with a Ti1-Ti2-Ti3-Ti4 dihedral angle of 35.7°. When the Ph-group in the β-diketonato ligand is replaced by another CF_3 group [16], the steric interactions are reduced and the Ti1-Ti2-Ti3-Ti4 dihedral angle changes to 14.1°. Two similar structures, one with R1 = R2 = CH_3 [38] and another with R1 = R2 = $C(CH_3)_3$ [39] were found in the literature; however the $(Ti\text{-}O)_4$-rings in both cases are planar as a result of the presence of crystallographically imposed symmetry operators.

Table 6. Comparison of O-C(R1)-C(R2)-O and Ti1-Ti2-Ti3-Ti4 dihedral angles

Substituent R1, R2	**O-C(R1)-C(R2)-O dihedral angle (°, av)**	**Ti1-Ti2-Ti3-Ti4 dihedral angle (°, av)**	**Reference**	**CCDC Refcode**
CF_3, Ph	4.0	35.7	Complex **4**	
CF_3, CF_3	2.0	14.1	16	VOYCET
CF_3, CF_3	4.3	-	40	XEYZAD
CH_3, CH_3	2.8	0	38	KUXVAA
$C(CH_3)_3$, $C(CH_3)_3$,	4. 7	0	39	RONBUR

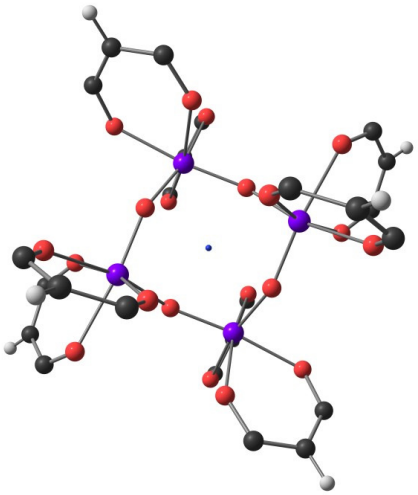

Figure 10. Structure of $[Ti(tfba)_2(\mu\text{-}O)]_4$ (4) with the Ph and CF_3 groups omitted. The eight β-diketonato backbones and the four bridging oxygens of the complex have S_4 molecular symmetry; the S_4 axis is perpendicular to the page at the blue dot. Color code of atoms (online version): Ti (purple), O (red), C (dark grey) and H (white).

3.6 Computational study of the $[Ti(tfba)_2Cl_2]$ + H_2biphen reaction.

It is reasonable to assume that the three cis-isomers of $[Ti(tfba)_2Cl_2]$ react with biphenol through a similar mechanism. This mechanism was explored with the major isomer observed in NMR studies (*cis-cis-trans* with Cl-cis, CF_3-cis, Ph-trans). We have previously analyzed the mechanism for a related complex, $[Ti(CH_3COCHCOCH_3)_2Cl_2]$, at the B3LYP level, with geometries optimized in vacuum [34]. Here we have employed solvent corrections to the geometries and energies (in form of the IEFPCM model, solvent = acetonitrile) and Grimme empirical dispersion corrections (D3) to reevaluate the mechanism. This change in computational protocol has profound consequences for the computed mechanism: whereas the gas phase B3LYP calculations indicated a highly concerted mechanism, where biphenol attack, Cl dissociation, and proton transfer from OH to Cl occur in a single step [34], the solvent calculations indicate that proton transfer occurs in a separate, low-barrier, step (Figure 11). Further, with dispersion corrections included in geometry optimizations, a distinct 7-coordinated intermediate can be found in the first reaction half (Inter1, Figure 12), indicating that biphenol attack and chloride dissociation are separate events. Frequency calculations confirm this intermediate as a stationary state on the potential energy surface. A distinct TS for biphenol-

association was not located. If dispersion corrections are removed from the computational protocol, the 7-coordinated intermediate collapses. Its formation is thus dependent on dispersion interactions. The formation of such an intermediate is supported by the NMR results indicating the formation of a 7-coordinated [Ti(tfba)$_2$Cl$_2$(CH$_3$CN)] species (Scheme 2). Once the 7-coordinated intermediate Inter1 is formed, the dissociation of chloride has little cost (~2.9 kcal/mol, TS$_{dissociation}$, Figure 13). Following chloride dissociation, the free chloride abstracts a proton from the free hydroxyl of the biphenol ligand, which simultaneously abstracts the proton from the Ti-coordinated hydroxyl (TS$_{proton1}$, Figure 11). The computed Gibbs free energies show that the proton transfer steps are underestimated (Figure 13), as has been observed earlier for other low-barrier proton transfer steps [41]. The formed Inter3 is low in energy and corresponds to the previously observed stable 6-membered reaction intermediate of a related reaction [34].

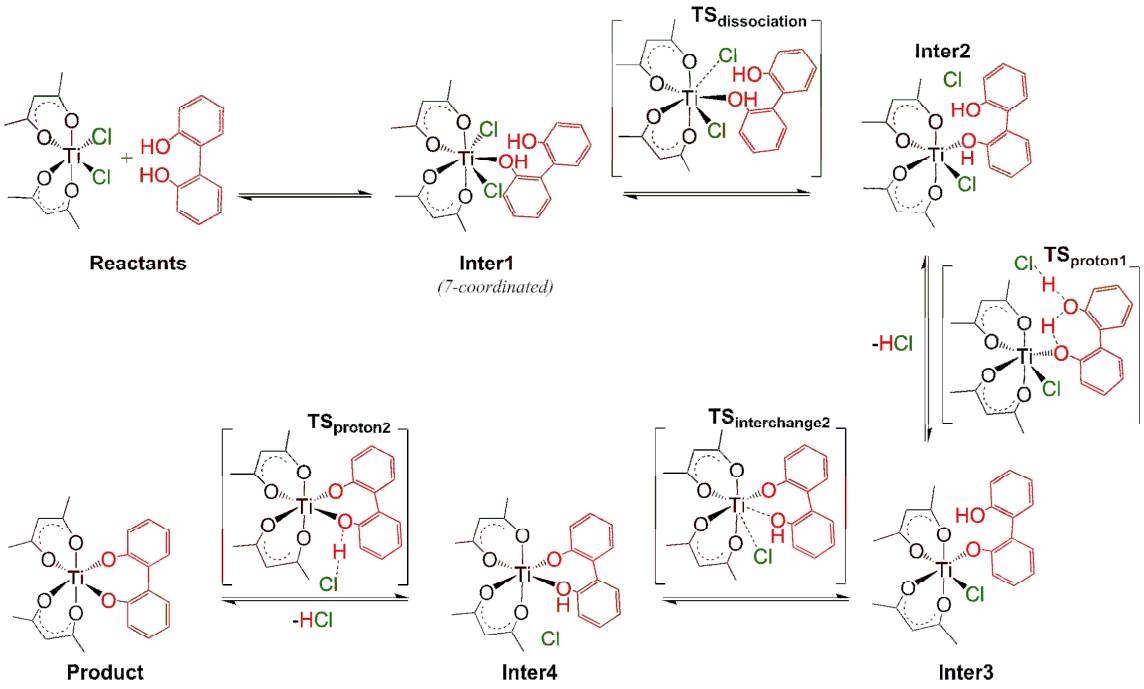

Figure 11. Mechanism for reaction of [Ti(PhCOCHCOCF$_3$)$_2$Cl$_2$] with biphenol as obtained from B3LYP-D3/IEFPCM computations. The CF$_3$ and Ph groups on the β-diketonato ligand are omitted in the figure.

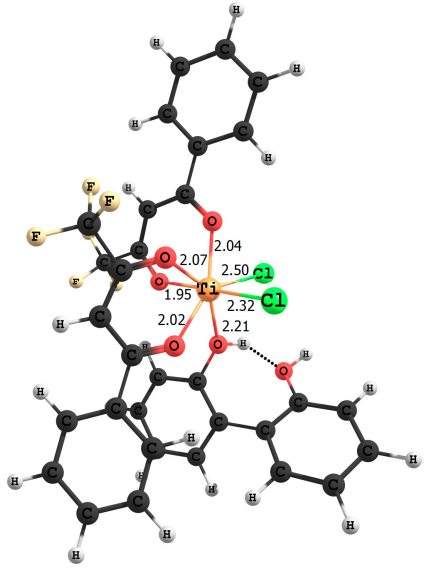

Figure 12. 7-coordinated intermediate (Inter1) formed in the reaction of $[Ti(PhCOCHCOCF_3)_2Cl_2]$ with biphenol as obtained from computations

Attack of the second hydroxy atom does not involve formation of a 7-coordinated species; instead an interchange mechanism with concerted dissociation of the second chloride ion is observed ($TS_{interchange}$, Figure 11). The second chloride substitution appears to be the slowest individual step ($TS_{interchange}$ with a barrier of 16.3 kcal/mol relative to Inter3), whereas the first chloride dissociation represents the highest point on the PES ($TS_{dissociation}$, 18.5 kcal/mol).

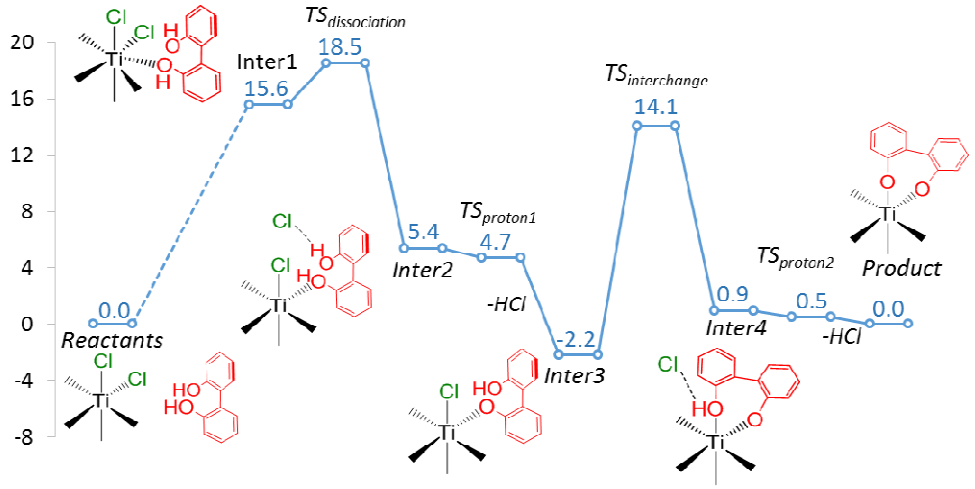

Figure 13. Gibbs free energies for the reaction of [Ti(PhCOCHCOCF$_3$)$_2$Cl$_2$] with biphenol, obtained at the B3LYP-D3/IEFPCM(acetonitrile)/6-311++G(2df,2p)//B3LYP-D3/IEFPCM(acetonitrile)/6-311G(d,p) level (including counterpoise and standard state corrections). The minima structures along the path are drawn schematically.

4 Conclusion

A study of the structure and properties of titanium(IV) complexes containing the oxygen-based β-diketonato ligand trifluorobenzoylacetonato, showed that [Ti(tfba)$_2$Cl$_2$] is susceptible to hydrolysis leading to dinuclear and tetranuclear complexes where the chlorines are substituted by bridged oxygens. However, substitution of the chlorines [Ti(tfba)$_2$Cl$_2$] with the electron-rich oxygen-based ligand H$_2$biphen gave [Ti(tfba)$_2$biphen] with enhanced hydrolytic stability. The substitution reaction occurs in two experimentally observed steps, each involving the substitution of a chlorine by an oxygen of the biphen^{2-} ligand. Computational chemistry calculations involving solvent and dispersion-corrected geometries show that the substitution of each chlorine requires several transition states, involving separate proton transfer steps and formation of a distinct 7-coordinated intermediate in the first reaction half.

5 Supporting Information

CCDC 1478542-1478543 contains the supplementary crystallographic data for **2** and **4**. These data can be obtained free of charge via http://www.ccdc.cam.ac.uk/conts/retrieving.html, or from the Cambridge Crystallographic Data Centre, 12 Union Road, Cambridge CB2 1EZ, UK; fax: (+44) 1223-336-033; or e-mail: deposit@ccdc.cam.ac.uk. Figure S1 and S2, Crystallographic data and DFT calculated optimized coordinates.

6 Acknowledgements

This work has received support from the South African National Research Foundation (JC, ML), the Central Research Fund of the University of the Free State (JC) and the University of Pretoria (ML),

and the Research Council of Norway through a Centre of Excellence Grant (Grant No. 179568/V30, KH) and a FRIPRO grant (Grant No. 23170/F20, KH). Grants of computer time from the Norwegian supercomputing program NOTUR are gratefully acknowledged: (Grant No. NN4654K, JC, KH and Grant No. NN9330K, KH)

7 References

[1] Palma, G.; D'Aiuto, M.; Rea, D.; Bimonte, S.; Lappano, R.; Sinicropi, M. S.; Maggiolini, M.; Longo, P.; Arra C.; Saturnino, C. Organo-Metallic Compounds: Novel Molecules in Cancer Therapy. *Biochem. Pharmacol.* **2014**, *3*, 1000149. DOI: 10.4172/2167-0501.1000149

[2] Meléndez, E.; Titanium complexes in cancer treatment. *Critical Reviews in Oncology/Hematology* **2002**, *42*, 309–315.

[3] Keppler, B. K.; Heim, M. E. Antitumor-active bis-β-diketonato metal complexes: budotitane – A new anticancer agent. *Drugs of the Future*, **1988**, *13*, 637–652.

[4] Immel T. A.; Groth, U.; Huhn, T. Őhlschläge P. Titanium Salan Complexes Displays Strong Antitumor Properties In Vitro and In Vivo in Mice. *PlosOne*, **2011**, *6*, e17869

[5] Schur, J.; Manna, C. M.; Tshuva, E. Y.; Ott, I. Quantification of the titanium content in metallodrugexposed tumor cells using HR-CS AAS. *Metallodrugs* **2014**; *1*, 1–9. DOI 10.2478/medr-2014-0001

[6] Sweeney NJ, Mendoza O, Müller-Bunz H, Pampillón C, Rehmann FJ, Strohfeldt K, Tacke M (2005). Novel benzyl substituted titanocene anti-cancer drugs. *Journal of Organometallic Chemistry* **690** (21-22): 4537–4544. doi:10.1016/j.jorganchem.2005.06.039.

[7] (a) Glasner, H.; Tshuva, E.Y. C1-Symmetrical Titanium(IV) Complexes of Salan Ligands with Differently Substituted Aromatic Rings: Enhanced Cytotoxic Activity, Inorg. Chem. 2014, 53, 3170−3176. DOI 10.1021/ic500001j

(b) Immel, T.A.; Grützke, M.; Spate, A.K.; Groth, U.; Ohlschlager, P.; Huhn, T. Synthesis and x-ray structure analysis of a heptacoordinate titanium(IV)-bis-chelate with enhanced *in vivo* antitumor efficacy. *Chem. Commun.* **2012**, *48*, 5790–5792.

(c) Immel, T.A.; Grützke, M.; Batroff, E.; Groth, U.; Huhn, T. Cytotoxic dinuclear titanium-salan complexes: Structural and biological characterization. *J. Inorg. Biochem.*, 2012, **106**, 68–75.

(d) Glasner, H.; Tshuva, E.Y. A marked synergistic effect in antitumor activity of salan titanium(IV) complexes bearing two differently substituted aromatic rings. *J. Am. Chem. Soc.* **2011**, *133*, 16812–16814. DOI 10.1021/ja208219f

(e) Tshuva, E.Y.; Peri, D. Modern cytotoxic titanium(IV) complexes; Insights on the enigmatic involvement of hydrolysis. *Coord. Chem. Rev.*, 2009, **253**, 2098–2115. doi:10.1016/j.ccr.2008.11.015.

(f) E.Y. Tshuva and J.A. Ashenhurst, Ti(IV) Complexes. Cytotoxic Titanium(IV) Complexes: Renaissanc. *Eur. J. of Inorg. Chem.*, 2009, **15**, 2203–2218. DOI: 10.1002/ejic.200900198.

[8] (a) Manna, C.M.; Braitbard, O.; Weiss, E.; Hochman, J.; Tshuva, E.Y. Cytotoxic salan-titanium(IV) complexes: High activity toward a range of sensitive and drug-resistant cell lines, and mechanistic insights. *ChemMedChem* **2012**, *7*, 703–708.

(b). Immel, T.A.; Grutzke, M.; Spate, A.K.; Groth, U.; Ohlschlager, P.; Huhn, T. Synthesis and x-ray structure analysis of a heptacoordinate titanium(IV)-bis-chelate with enhanced *in vivo* antitumor efficacy. *Chem. Commun.* **2012**, *48*, 5790–5792.

[9] (a) M. Shavit, D. Debiak, C. M. Manna, J. S. Alexander, E. Y. Tshuva, J. Active Cytotoxic Reagents Based on Non-metallocene Non-diketonato Well-Defined C_2-Symmetrical Titanium Complexes of Tetradentate Bis(phenolato) Ligands, *J. Am. Chem. Soc*. 2007, 129, 12098 – 12099. DOI: 10.1021/ja0753086

(b) D. Peri, S. Meker, M. Shavit, E. Y. Tshuva, Synthesis, Characterization, Cytotoxicity, and Hydrolytic Behavior of C_2- and C_1-Symmetrical Ti^{IV} Complexes of Tetradentate Diamine Bis(Phenolato) Ligands: A New Class of Antitumor Agents, *Chem. Eur. J*. 2009, 15, 2403 – 2415, DOI: 10.1002/chem.200801310

[10] Boyle, T. J.; Pearson, A. T.; Schwartz, R. W. Synthesis and Characterization of Group IV Metal Adamantanol Alkoxides as Potential PZT Precursors. *Ceram. Trans.*, 1994, **43**, 79.

[11] Corden, J. P.; Errington, W.; Moore, P.; Partridge, M. G.; Wallbridge, M. G. H. Synthesis of di-, tri- and penta-nuclear titanium(IV) species from reactions of titanium(IV) alkoxides with 2,2′-biphenol (H_2L^1) and 1,1′-binaphthol (H_2L^2); crystal structures of $[Ti_3(\mu 2\text{-}OPri)_2(OPri)_8L^1]$, $[Ti_3(OPri)_6L^1{}_3]$, $[Ti_5(\mu_3\text{-}O)_2(\mu_2\text{-}OR)_2(OR)_6L^1{}_4]$ (R = OPr^i, OBu^n) and $[Ti_2(OPr^i)_4L^2{}_2]$, Dalton Trans., 2004, 1846-1851. DOI: 10.1039/B404197F.

[12] Aizwa, M.; Nosaka, Y.; Fujii, N. FT-IR liquid attenuated total reflection study of TiO_2-SiO_2 sol-gel reaction. *J. Non-Cryst. Solids*. **1991**, *128*, 77-85. doi:10.1016/0022-3093(91)90778-5

[13] W.A. Collier, F. Krauss, Zeitschrift für Krebsforschung, 1931, 34, 527

[14] Furniss, B. S.; Hannaford, A. J.; Smith, P. W. G.; Tatchell, A. R. Vogel's Textbook of Practical Organic Chemistry, 5th ed.; John Wiley & Sons: New York, **1994**, 409.

[15] Kuhn, A.; Tsotetsi, T. A.; Muller, A.; Conradie, J. Isomer Distribution and Structure of (2,2'-Biphenyldiolato)bis(β-diketonato)titanium(IV) Complexes: a Single Crystal X-ray, Solution NMR and Computational Study, *Inorg. Chim. Acta.,* **2009**, 362, 3088-3096. DOI 10.1016/j.ica.2009.02.006.

[16] Kuhn, A.; Conradie, J. Observed hydrolysis of fluorine substituted bis(β-diketonato)-dichlorotitanium(IV) complexes. Dalton Trans. **2015**, *44*, 5106–5113. DOI: 10.1039/C4DT02614D

[17] Espenson, J. H. in: Chemical Kinetics and Reaction Mechanisms 2nd ed., McGraw-Hill, New York, 1995, pp. 15, 49, 70-75, 156.

[18] Helm, L. MINSQ, Non-Linear parameter estimation and model development, least squares parameter optimization, V3.12; MicroMath Scientific Software: Salt Lake City, UT, (1990).

[19] Gaussian 09, Revision D.01, Frisch, M. J.; Trucks, G. W.; Schlegel, H. B.; Scuseria, G. E.; Robb, M. A.; Cheeseman, J. R.; Scalmani, G.; Barone, V.; Mennucci, B.; Petersson, G. A.; Nakatsuji, H.; Caricato, M.; Li, X.; Hratchian, H. P.; Izmaylov, A. F.; Bloino, J.; Zheng, G.; Sonnenberg, J. L.; Hada, M.; Ehara, M.; Toyota, K.; Fukuda, R.; Hasegawa, J.; Ishida, M.; Nakajima, T.; Honda, Y.; Kitao, O.; Nakai, H.; Vreven, T.; Montgomery, J. A., Jr.; Peralta, J. E.; Ogliaro, F.; Bearpark, M.; Heyd, J. J.; Brothers, E.; Kudin, K. N.; Staroverov, V. N.; Kobayashi, R.; Normand, J.; Raghavachari, K.; Rendell, A.; Burant, J. C.; Iyengar, S. S.; Tomasi, J.; Cossi, M.; Rega, N.; Millam, J. M.; Klene, M.; Knox, J. E.; Cross, J. B.; Bakken, V.; Adamo, C.; Jaramillo, J.; Gomperts, R.; Stratmann, R. E.; Yazyev, O.; Austin, A. J.; Cammi, R.; Pomelli, C.; Ochterski, J. W.; Martin, R. L.; Morokuma, K.; Zakrzewski, V. G.; Voth, G. A.; Salvador, P.; Dannenberg, J. J.; Dapprich, S.; Daniels, A. D.; Farkas, Ö.; Foresman, J. B.; Ortiz, J. V.; Cioslowski, J.; Fox, D. J. Gaussian, Inc., Wallingford CT, 2009.

[20] Grimme, S.; Antony, J.; Ehrlich, S.; Krieg, H.; A consistent and accurate ab initio parametrization of density functional dispersion correction (DFT-D) for the 94 elements H-Pu. *J. Chem. Phys*. **2010**, ***132*****,** 154104. doi.org/10.1063/1.3382344

[21] (a) Tomasi, J.; Mennucci, B.; Cammi, R. Quantum Mechanical Continuum Solvation Models. *Chem. Rev.* **2005**, *105*, 2999-3094, DOI: 10.1021/cr9904009 (b) Tomasi, J.; Mennucci, B.; Cancès E. J. The IEF version of the PCM solvation method: an overview of a new method addressed to study molecular solutes at the QM ab initio level. *J. Mol. Struct. (Theochem)* **1999**, *464*, 211-216, (c) Cancès, E.; Mennucci, B.; Tomasi, J. A new integral equation formalism for the polarizable continuum model: Theoretical background and applications to isotropic and anisotropic dielectrics. *J. Chem. Phys.* **1997**, *107*, 3032-3041. doi.org/10.1063/1.474659

[22] APEX2 (including SAINT and SADABS); Bruker AXS Inc., Madison, WI (2012).
[23] Sheldrick, G. M. A short history of SHELX. *Acta Crystallogr.* **2008**, *A64*, 112-122.
[24] Farrugia, L. J. ORTEP-3 for Windows - a version of ORTEP-III with a Graphical User Interface (GUI), *J. Appl. Crystallogr.* **1997,** *30*, 565. doi:10.1107/S0021889897003117
[25] Keppler B.K., Hartmann M., New Tumor-Inhibiting Metal Complexes. Chemistry and Antitumor Properties, Metal-Based Drugs, 1 (1994) 145-149. doi: 10.1155/MBD.1994.145
[26] Bradley, D. C.; Holloway, C. E.; Nuclear magnetic resonance and infrared spectral studies on labile cis-dialkoxy-bis(acetylacetonato)titanium(IV) compounds. *J. Chem. Soc. A.* **1969**, 282-285.
[27] (a) B.K. Keppler, C. Friesen, H.G. Moritz, H. Vongerichten, E. Vogel, in Metal Complexes in Cancer Chemotherapy, B.K. Keppler, (ed.) VCH: Weinheim, Germany, **1993**, pp. 297. (b) P. Comba, H. Jakob, B. Nuber, B.K. Keppler, Solution Structures and Isomer Distributions of Bis(β-diketonato) Complexes of Titanium(IV) and Cobalt(III). *Inorg. Chem.* **1994**, 33, 3396-3400.
[28] (a) Fay, R. C.; Lowry, R. N. Stereochemistry and lability of dihalobis(.beta.-diketonato)titanium(V) complexes. I. Acetylacetonates. *Inorg. Chem.* **1967**, 6, 1512-1519;
(b) Serpone, N.; Fay, R. C. Stereochemistry and lability of dihalobis(.beta.-diketonato)titanium(IV) complexes. II. Benzoylacetonates and dibenzoylmethanates. *Inorg. Chem.* **1967**, 6, 1835-1843;
(c) Fay, R. C.; Lowry, R. N. Proton magnetic resonance studies of ligand-exchange equilibriums for dihalo- and diethoxybis(.beta.-diketonato)titanium(IV) complexes. *Inorg. Chem.* **1974**, 13, 1309-1313.
[29] Bradley, D. C.; Holloway, C. E. Some labile cis-dialkoxybis(acetylacetonato)titanium compounds. *Chem. Commun. (London),* **1965**, 284-284. DOI: 10.1039/C19650000284.
[30] (a) Harrod, J. F.; Taylor, K. Intramolecular rearrangement in some bis(chelate)titanium(IV) complexes. *J. Chem. Soc. D,* **1971**, 696-697. DOI: 10.1039/C29710000696.
(b) Baggett, N.; Poolton, D. S. P.; Jennings, W. B. Nuclear magnetic resonance investigation of the dynamic stereochemistry of some octahedral titanium(IV) chelate complexes. *J. Chem. Soc., Chem Commun.* **1975**, 239-240.
(c) Baggett, N.; Poolton, D. S. P.; Jennings, W. B. A comparative dynamic nuclear magnetic resonance study of degenerate enantiomerization and dionate site exchange in octahedral diolatobis(pentane-2,4-dionato)titanium(IV) complexes. *J. Chem. Soc. Dalton Trans.* **1979**, 1128-1134.
(d) Fay, R. C.; A.F. Linmark, Dynamic nuclear magnetic resonance studies of inversion and diketonate R-group exchange in dialkoxybis(.beta.-diketonato)titanium(IV) complexes. *J. Am. Chem. Soc.*, **1975**, *97*, 5928-5930.
(e) Finocchiaro, P. Direct evidence for reversal of helicity in the stereoisomerization mechanism of bis(β-diketonato)titanium(IV) complexes. *J. Am. Chem. Soc.*, **1975**, *97*, 4443-4444.
(f) Serpone, N.; Bickley, D. G. Configurational rearrangements in *cis*-$M(AA)_2X_2$, *cis*-$M(AA)_2XY$, and *cis*-$M(AB)_2X_2$ complexes. 5. The *cis*-$M(AA)_2X_2$ system - diastereotopic probe on the monodentate X ligands. *Inorg. Chim. Acta*, **1979**, *32*, 217-228.
(g) Bickley, D. G.; Serpone, N. Configurational rearrangements in cis-$M(AA)_2X_2$, cis-$M(AA)_2XY$, and cis-$M(AB)_2X_2$ complexes. 6. Bis(chelate)bis(2,6-diisopropylphenoxy)titanium systems (chelate = acetylacetonate, 8-hydroxyquinolinate, and 8-hydroxyquinaldinate). Inorg. Chem., **1979**, *18*, 2200-2204.
(h) Serpone, N.; Bickley, D. G. Configurational rearrangements in *cis*-$M(AA)_2X_2$, *cis*-$M(AA)_2XY$, and *cis*-$M(AB)_2X_2$ complexes. 10. The *cis*-$M(AB)_2X_2$ system - diastereotopic probe on the X ligands. *Inorg. Chim. Acta*, **1982**, *57*, 211-216.
[31] (a) Thompson, D. W.; Somers W. A.; Workman, M. O. Complexes of titanium(IV) containing the 3-methyl-2,4-pentanedionate anion. *Inorg. Chem.* **1970**, *9*, 1252-1254.
(b) Linmark, A. F.; Fay, R. C. Dipseudohalobis (.beta.-diketonato)titanium(IV) complexes. Synthesis, stereochemistry, configurational rearrangements, and vibrational spectra. *Inorg. Chem.* **1975**, *14*, 282-287.
(c) Bickley, D. G.; Serpone, N. Configurational rearragements in *cis*-$M(AA)_2X_2$, *cis*-$M(AA)_2XY$, and cis-$M(AB)_2X_2$ complexes. 4. The *cis*-$M(AA)_2X_2$ system: $Ti(3\text{-}^{i}C_3H_7\text{-acac})_2Cl_2$. *Inorg. Chim.*

Acta, **1977**, *25*, L139-L141.
(d) Wilkie, C. A.; Lin, G.-Y.; Haworth, D.T. A comparative study of the cis-disubstituted bis(β-diketonato) titanium(IV) complexes. *J. Inorg. Nucl. Chem.*, **1978**, *40*, 1009-1012.
(e) Bickley, D. G.; Serpone, N. Configurational rearrangements in *cis*-$M(AA)_2X_2$, *cis*-$M(AA)_2XY$, and 3. The *cis*-$M(AA)_2X_2$ system - diastereotopic probe on the terminal AA groups [1, 2]. *Inorg. Chim. Acta*, **1978**, *28*, 169-175.
(f) Bickley, D. G.; Serpone, N. Configurational rearrangements in *cis*-$M(AA)_2X_2$, *cis*-$M(AA)_2XY$ and *cis*-$M(AB)_2X_2$ complexes. 7. The cis-$M(AA)_2XY$ system - diastereotopic probe on AA [1]. *Inorg. Chim. Acta*, **1980**, *38*, 177-181.
(g) Bickley, D. G.; Serpone, N. Configurational rearrangements in *cis*-$M(AA)_2X_2$, *cis*-$M(AA)_2XY$ and *cis*-$M(AB)_2X_2$ complexes. 8. The cis-$M(AA)_2XY$ system, Y = $O^iC_3H_7$ and 2,6-$(^iC_3H_7)_2C_6H_3O$. *Inorg. Chim. Acta*, **1980**, *40*, 213-216.
(h) Bickley, D. G.; Serpone, N. Configurational rearrangements in *cis*-$M(AA)_2X_2$, *cis*-$M(AA)_2XY$ and *cis*-$M(AB)_2X_2$ complexes 9. The cis-$M(AB)_2X_2$ System - diastereotopic probe on AB. *Inorg. Chim. Acta*, **1980**, *43*, 185-189.

[32] Kuhn, A.; Conradie, J. Structural investigation of trifuoromethyl substituted bis(β-diketonato)-dichlorotitanium(IV) complexes displaying a mono-dinuclear equilibrium hydrolysis reaction. Journal of Molecular Structure **2015**, *1089*, 267–276. DOI: 10.1016/j.molstruc.2015.06.017

[33] Fay, R.C.; Lowry, R.N. Preparation and characterization of diiodobis(acetylacetonato)titanium(IV). *Inorg. Chem*. **1970**, *9*, 2048-2052.

[34] Hopmann, K. H.; Kuhn, A.; Conradie, J. Substitution reactions of dichlorobis(betadiketonato-*O,O'*) titanium(IV) complexes with aryl diolato ligands: an experimental and computational study. *Polyhedron*, **2014**, *67*, 231-241. DOI: 10.1016/j.poly.2013.09.004

[35] Burgess, J.; Parson, S. A.; Kinetics of substitution at ternart titanium(IV)-cyclopentadienyl, pyronato or pyridinato-halide or alkoxide complexes. *Applied Organomet. Chem.* **1993**, *7*, 343-351.

[36] Tsotetsi, T.A., Kuhn, A., Muller, A. and Conradie, J. Substitution kinetics of biphenol at dichlorobis(2,4-pentadionato-κ^2O,O')titanium(IV): Isolation, Characterization, Crystal Structure and Enhanced Hydrolytic Stability of the Product (2,2'-Biphenyldiolato)bis(2,4-pentadionato-κ^2O,O')titanium(IV). *Polyhedron,* **2009**, 28, 209-214. DOI 10.1016/j.poly.2008.10.025.

[37] Kongprakaiwoot N.; Quiroz-Guzman, M.; Oliver, A. G. and Brown, S. N. Gauging electronic dissymmetry in bis-chelates of titanium(IV) using sterically and electronically variable 2,2'-biphenoxides. *Chem. Sci.*, **2011**, 2, 331 – 336. DOI: 10.1039/c0sc00468e.

[38] Jeske, P., Wieghardt, K. and Nuber, B. Synthesis, Crystal Structure and 'H N M R Spectrum of the Tetranuclear Complex $[\{LT0i(0CH_3)\}_2(\mu\text{-}0)_4\{Ti(acac)_2\}_2](C10_4)_2 \bullet 2H_20$. *Z. Naturforsch. ,B: Chem. Sci.* **1992**, 47(b), 1621-1627.

[39] Troyanov, S. I. and Gorbenko, O. Y. Crystal and molecular structure of cyclotetrakis[μ-oxo-bis(2,2,6,6-tetramethylheptan-3,5-dionate)titanium(IV)] pentane adduct. *Polyhedron,* **1997**, 16(5), 777-780.

[40] Kuhn, A., Muller, A. and Conradie, J. μ-2,2′-Biphenolato-κ^2*O:O'*-μ-oxido-κ^2*O:O*-bis[bis-(hexafluoroacetylacetonato-κ^2*O,O'*)titanium(IV)]. *Acta Cryst.* **2007**, E63, m664-m666. doi:10.1107/S1600536807004588.

[41] a) Hopmann, K. H.; Himo, F. Theoretical Study of the Full Reaction Mechanism of Human Soluble Epoxide Hydrolase. *Chem. Eur. J.* **2006**, 12, 6898-6909. DOI: 10.1002/chem.200501519
b) Hopmann, K.H., Full Reaction Mechanism of Nitrile Hydratase: A Cyclic Intermediate and an Unexpected Disulfide Switch. *Inorg. Chem.* **2014**, *53*, 2760-2762